We are IntechOpen,
the world's leading publisher of
Open Access books
Built by scientists, for scientists

6,900
Open access books available

185,000
International authors and editors

200M
Downloads

154
Countries delivered to

Our authors are among the

TOP 1%
most cited scientists

12.2%
Contributors from top 500 universities

CLARIVATE ANALYTICS

BOOK CITATION INDEX

INDEXED

WEB OF SCIENCE™

Selection of our books indexed in the Book Citation Index
in Web of Science™ Core Collection (BKCI)

Interested in publishing with us?
Contact book.department@intechopen.com

Numbers displayed above are based on latest data collected.
For more information visit www.intechopen.com

Autobioluminescent Cellular Models for Enhanced Drug Discovery

Tingting Xu, Michael Conway, Ashley Frank,
Amelia Brumbaugh, Steven Ripp and Dan Close

Additional information is available at the end of the chapter

Abstract

Autobioluminescent cellular models are emerging tools for drug discovery that rely on the expression of a synthetic, eukaryotic-optimized luciferase that does not require an exogenous chemical substrate to produce its resultant output signal. These models can therefore self-modulate their output signals in response to metabolic activity dynamics and avoid the sample destruction and intermittent data acquisition limitations of traditional fluorescent or chemically stimulated bioluminescent approaches. While promising for reducing drug discovery costs and increasing data acquisition relative to alternative approaches, these models have remained relatively untested for drug discovery applications due to their recent emergence within the field. This chapter presents a history and background of these autobioluminescent cellular models to offer investigators a generalized point of reference for understanding their capabilities and limitations and provides side-by-side comparisons between autobioluminescent and traditional, substrate-requiring toxicology screening platforms for pharmaceutically relevant three-dimensional and high-throughput screening applications to introduce investigators to autobioluminescence as a potential new drug discovery toolset.

Keywords: luciferase, *lux*, toxicology, high-throughput screening, three-dimensional cell culture, drug discovery

1. Introduction to autobioluminescence

1.1. A brief overview of autobioluminescence

Autobioluminescence is defined as the ability of a cell to self-initiate the production of a luminescent signal using only endogenously supplied substrates to perform the enzymatic reactions necessary for signal generation. In this regard, it is separate from traditional bioluminescence in that it is not dependent on the exogenous addition of a chemical substrate to supplement the metabolic cosubstrates that are naturally present within cells expressing an associated luciferase protein. Interestingly, under this definition, there are many examples of autobioluminescence in nature that can be found across a diverse array of organisms such as bacteria, dinoflagellates, fungi, and beetles [1]. However, of these natural autobioluminescent systems, only that of the bacteria (commonly referred to as the *lux* system) has been successfully transitioned as a reporter system for scientific applications while maintaining its autonomous functionality [2–4]. The remaining systems, such as firefly luciferase, *Renilla* luciferase, and *Gaussia* luciferase, have been limited in this transition by incomplete understandings of the genetic frameworks behind their substrate production biochemical pathways or limitations on the abilities of host cells to support the endogenous production of all the components required for their expression. These systems therefore all require the external application of a chemical substrate (D-luciferin for firefly luciferase and coelenterazine for *Renilla* and *Gaussia* luciferase) to activate their light production under scientifically relevant applications [5].
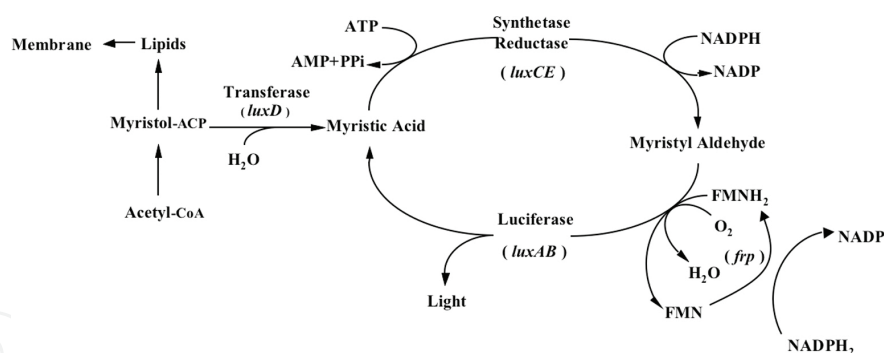
Figure 1. The autobioluminescent reaction catalyzed by the bacterial luciferase gene cassette. The luciferase is formed from a heterodimer of the *luxA* and *luxB* gene products. The aliphatic aldehyde is supplied and regenerated by the products of the *luxC*, *luxD*, and *luxE* genes. The required oxygen and reduced riboflavin phosphate substrates are scavenged from endogenous metabolic processes and the flavin reductase gene (*frp*) aids in reduced flavin turnover rates in some species. Used with permission from [7] under a Creative Commons Attribution-Noncommercial license.

The successfully transitioned bacterial *lux* system, alternatively, utilizes a characterized core set of five genes, *luxC*, *luxD*, *luxA*, *luxB*, and *luxE*, to express both its luciferase enzyme (a dimer formed by the *luxA* and *luxB* gene products) and its supporting transferase (*luxD*), reductase (*luxC*), and synthetase (*luxE*) enzymes that supply the required aldehyde substrate from natural cellular metabolic components. In addition, this reaction also requires the metabolites $FMNH_2$ and O_2 in order to function, producing a luminescent output at 490 nm and a

reduced corresponding acid compound, FMN, and H_2O as products [6] (**Figure 1**). Interestingly, despite the relatively straightforward organization of this system and the longstanding elucidation of its individual components roles and genetic identities, there were significant hurdles that needed to be overcome before it could be successfully transitioned for expression in the mammalian systems that are required for drug discovery applications.

1.2. History of autobioluminescent cellular model development

Due to its bacterial origin, the *lux* cassette was formerly believed to function solely in prokaryotic hosts, and thus was not considered a viable tool for diagnostic screening in human cell lines [8]. This belief was due to the initial difficulty researchers encountered in coordinating the temporal and spatial coexpression of the multiple *lux* genes, the thermoinstability of the *lux* proteins at the mammalian optimal temperature of 37°C, and the limited availability of the $FMNH_2$ cosubstrate within human cells relative to their uncompartmentalized bacterial counterparts. As a result of these initial difficulties, alternative bioluminescent systems became more popular for use in drug discovery applications. In particular, firefly luciferase (*luc*) has become the dominant bioluminescent imaging target for this application due to its single gene expression requirement, high quantum yield, and favorable output signal wavelength of 562 nm [9].

However, despite the initial challenges associated with transitioning the bacterial *lux* system into mammalian cells, significant progress was made over the years that would eventually lead to the development of an optimized version of the system that could function reliably within the human cellular microenvironment. The first major stepping stone in this process was the expression of a functional luciferase heterodimer (*luxAB*) in the human kidney cell line HEK293 by Patterson et al. in 2005 [10]. This demonstration was particularly important because Patterson and her colleagues were able to overcome the previous limitations of both spatial/temporal coexpression and protein thermostability. Unlike previous work that had attempted to coordinately express the genes using short protein linker sequences or individual promoters [11–16], Patterson et al. linked the *luxA* and *luxB* genes using an internal ribosomal entry site (IRES) element to allow for expression of individual protein products from a single mRNA transcript. Thermostability issues were overcome by using human codon optimized gene sequences corresponding to the less utilized *Photorhabdus luminescens* bacterial system, which allowed for higher levels of transgene expression of proteins with greater thermal tolerance than those of the traditionally employed *Aliivibrio fischeri* (previously *Vibrio fischeri*) system [17].

Further advances were made to the *lux* system by Close et al. in 2010 that built heavily upon the techniques developed by Patterson et al. [18]. This later work expanded the earlier IRES-based expression strategy to coexpress pairs of *lux* genes from individual promoters and divide the expression of the genes across two plasmids. Most importantly, however, Close and his colleagues were able to overcome the limitation of signal output strength imparted by the low level of endogenously available $FMNH_2$ by including a sixth gene (*frp*) that encoded for a flavin reductase enzyme. This enzyme was able to rapidly recycle the oxidized FMN in the mammalian cytosol into $FMNH_2$, which increased light output to the point where it could be visualized externally using commonly available detection equipment. This marked the first

demonstration of autobioluminescence in a host system amenable to drug discovery applications, however, the autobioluminescent output levels from this approach were significantly lower than traditional bioluminescent systems and the use of multiple plasmids and large, repetitive IRES element DNA sequences made the system difficult to work with on a molecular biology level.

These difficulties were later overcome by Xu et al. in 2014, who re-optimized the system for expression from a single promoter and therefore allowed it to be expressed from a single plasmid [19]. This approach, which substituted viral 2A elements in place of the previously employed IRES elements, allowed the full autobioluminescent DNA cassette to be manipulated as a single gene and significantly increased the signal output level to the point where it could be detected from the low numbers of cells that are commonly used in high throughput screening applications. Using the new expression format, Xu and her colleagues were able to demonstrate the use of autobioluminescent reporters for tracking cellular metabolic dynamics, population sizes, and promoter activation events, finally demonstrating the use of autobioluminescence for the same applications as traditional bioluminescent reporter systems [19, 20].

1.3. Comparison of autobioluminescent, traditional bioluminescent, and fluorescent optical imaging approaches

Unlike alternative bioluminescent and fluorescent reporter systems, which have been widely employed for drug discovery for many years, the autobioluminescent system is relatively new and thus has not been used by as many investigators as have the traditional systems. It is therefore important to briefly define the primary differences between these systems and detail the advantages and disadvantages of each as potential optical imaging targets. Fluorescent systems, with green fluorescent protein (*gfp*) being the most recognizable example, are arguably the most familiar of the optical imaging approaches and have several significant advantages in that they are small, single gene constructs that are simple to introduce into cells, do not require chemical exposure or sample destruction to function, and are available in a wide variety of excitation and emission wavelengths to suit individual assay needs [21]. Their primary drawback is that their requisite excitation signals can result in autofluorescent background signals from the cells or subjects under study, often requiring specialized equipment to filter out undesired light in order to acquire the resultant emission signal [22]. In addition, complications can arise from the prolongation of fluorescent protein activity after transcription has been stopped (enzymatically or through cell death) and phototoxicity to host cells, yielding inaccurate readings in toxicity or metabolic activity assays.

Bioluminescent reporters, on the other hand, express high signal-to-noise ratios due to the near absence of natural bioluminescent production from host tissues and can be sourced from a variety of different organisms with different substrates and output wavelengths to allow for reporter multiplexing within a single system. However, similar to fluorescent reporters, the luciferase proteins can remain active following genetic downregulation or cell death. In addition, the introduction of the activating chemical substrate has the potential to unexpect-

edly influence the cellular system under study and requires the destruction of the sample to efficiently interact with the genetically expressed luciferase [23].

Autobioluminescent reporters somewhat bridge these two systems by combining the favorable high signal-to-noise ratios of traditional bioluminescent systems and the nondestructive nature of the fluorescent systems. However, while their reliance on only endogenously produced substrates eliminates concerns over phototoxicity or substrate interference, it also reduces their total bioluminescent output levels relative to chemically stimulated systems. In addition, there is currently only a single variant, and thus only a single output signal wavelength, available for use [24]. Therefore, in the absence of a system that overcomes all limitations, investigators must weigh the pros and cons of each approach to determine which is the most appropriate for gathering their required data.

2. The use of autobioluminescent cellular models for high throughput compound screening

2.1. Advantages of autobioluminescent cellular models for high throughput screening

Despite their output limitations relative to chemically stimulated bioluminescent systems, autobioluminescent cellular models are particularly well suited for cytotoxicity assays and tier I drug development screening because of their ability to endogenously synthesize and regenerate the luminogenic substrates and cofactors ($FMNH_2$ and O_2) required for light production. This autonomous signal production potential eliminates costly reagents and minimizes the complexity of traditional assays formats, offering a simplified and cost-effective high throughput approach that reduces hands-on human interaction and error. In practice, the inherent high signal-to-noise ratio of the autobioluminescent signal is able to overcome the relatively reduced total output flux to allow these models to function similarly to their chemically stimulated counterparts [19, 25, 26]. This provides a significant advantage for their use in *in vitro* high throughput viability assays, which have traditionally been fluorescence based and are complicated by high background interference from cellular heme compounds and tissue culture supplements [26–29]. This reduction in background has allowed autobio-luminescent cellular models to be applied as counterscreens for identifying false positives in assays with notoriously high background effects, as was recently demonstrated in a study to assess the rate of false positives in a fluorescence-based assay for detecting the Alzheimer's-implicated Tau protein [30].

While this low background advantage is shared by traditional bioluminescent cellular models, the unstimulated production of light that is unique to the autobioluminescent system provides an additional advantage in that it allows for longitudinal data acquisition without sample destruction. The presence of a continuous output signal that can represent real-time metabolic activity dynamics offers enhanced temporal resolution for assaying the cytotoxicity of therapeutic compounds in high throughput screening formats and provides for standardization without the need to tailor each assay to the unknown kinetics of novel compounds [19].

The typical chemically stimulated, bioluminescent-based *in vitro* high throughput screening assay requires an average of five sacrificial time points to generate sufficient data for understanding the cytotoxicity of a compound. To take advantage of the full throughput capacity of a 1536-well plate, this requires the preparation, treatment, and processing of 7680 samples. However, the nondestructive nature of the autobioluminescent testing format reduces these sample requirements to only a single plate (1536 samples), which can then be imaged repeatedly at each time point. This eliminates the generation, maintenance, and treatment of 6144 samples over the course of a typical assay, and thus greatly reduces financial costs while increasing the convenience and quality of kinetic data collection.

2.2. Previously published examples of autobioluminescent cellular models for high throughput screening

Because of the reduction in cost and complexity and increase in data acquisition afforded by continuous imaging, autobioluminescent cellular models are becoming increasingly employed as tools for early stage therapeutic compound cytotoxicity screening. Recently, researchers at the National Institutes of Health performed a competitive evaluation of autobioluminescent and commonly applied ATP content, alamarBlue, CyQUANT, and MTS metabolic activity assays using a multi-time point study approach and reported that the IC_{50} data of known cytotoxic compounds were consistent across each system [25]. In this comparison, the continuous data output of the autobioluminescent cellular models was specifically investigated by comparing a single sample set against individually prepared sample sets that were sacrificed at each time point, and it was determined that repeated assessment of a single sample correlated well with the individually prepared samples of the alternative assays.

More in-depth comparisons have also been performed that contrasted the use of autobioluminescent and chemically stimulated bioluminescent reporter systems to assess the pharmacological effects of compounds on human cellular models *in vitro*. In this evaluation, the autobioluminescent models were compared with a chemically stimulated bioluminescent ATP content assay following exposure of cells to the Library of Pharmacologically Active Compounds (LOPAC), which contains 1280 compounds known to possess pharmacologically active effects on human tissues. When deployed in a high throughput 1536-well format, the IC_{50} data from the autobioluminescent cellular models yielded a strong correlation to the results of the ATP assay ($R^2 = 0.7847$), but with the added strength of allowing for kinetic monitoring, thus showcasing its power as a biomonitoring tool for cell toxicity and compatibility with high throughput conditions. While this study focused on the HEK293 human kidney cell line, the same advantages should remain applicable in more medically relevant drug screening models as well [19].

2.3. Incorporation of autobioluminescent cellular models into existing drug discovery workflows

Although it has not been the primary focus of any previously published autobioluminescent work, an interesting observation from the existing literature is that autobioluminescent cellular models can often be substituted into existing bioluminescent and fluorescent assay

workflows without significant changes to the original assay protocols. This interoperability results from the similarity of the autobioluminescent output signal to those from the chemically simulated bioluminescent systems for which the protocols and existing detection equipment were originally designed. Because in both cases the output signals are light in the visible wavelength, the only major considerations when switching between systems have been the variation in output signal intensity and the necessary imaging parameter adjustments needed to achieve minimum signal detection thresholds. This minimizes the level of hardware optimization required to shift between assay modalities in both *in vitro* and *in vivo* imaging protocols.

A review of the literature suggests that the primary method for optimizing minimum signal detection thresholds during this transition has been to employ larger numbers of cells to overcome the difference in signal output between chemically stimulated and autobioluminescent systems. In autobioluminescent systems, signal detection has been demonstrated from population sizes down to 20,000 cells/well in a 24-well plate format, and from as few as 25,000 cells following subcutaneous injection into a mouse model [18]. While these are significantly larger numbers of cells than are required for chemically stimulated bioluminescent systems, the low background associated with bioluminescence has nonetheless been shown to retain sufficient sensitivity for use in whole-animal imaging experiments [28, 31]. It is important to note, however, that in some cases the use of increased cell numbers is not possible, such as for studies specifically focused on very small numbers of cells, such as early stage colonizing tumors. In these scenarios, the primary optimization employed must focus on adjustment of the imaging parameters, such as the use of longer acquisition times or increased luminescent pixel binning sizes.

3. Correlating the data output of autobioluminescent cellular models to classical assay formats

Since the generation of autobioluminescence relies upon the cell's capability to express the synthetic bacterial luciferase cassette as well as the availability of endogenous metabolites (e.g., O_2 and $FMNH_2$) for the synthesis of the required substrates, the autobioluminescent light output of these models correlates very strongly with the overall cellular metabolic activity level. As such, autobioluminescent cellular models represent excellent indicators for cytotoxicity following exposure to a compound of interest. Unlike conventional cytotoxicity assays that often require cellular destruction concurrent with data acquisition, autobioluminescent cellular models continuously self-modulate their light output in response to metabolic activity dynamics across the full lifetime of the host, thus allowing for the noninvasive visualization of metabolic activity at any time point throughout the entire exposure period. As a result, the nondestructive autobioluminescence assay generates more data similar to that obtained by traditional assays while simultaneously reducing the number of samples and investigator interaction time required per run. As an example of these capabilities, a side-by-side comparison between an autobioluminescent HEK293 cell model and the classic 3-(4,5-dimethylthiazol-2-yl)-2,5-diphenyltetrazolium bromide (MTT) cytotoxicity assay was performed over a 96-

hour exposure period. In this evaluation, the autobioluminescent model system demonstrated similar toxicity response data across the full set of compound exposure concentrations, and correlated strongly with the MTT assay (R^2 = 0.9262 at 96-hour postexposure) (**Figure 2A**). Similarly, a strong correlation (R^2 = 0.9163) was obtained between the autobioluminescent model system and an ATP content-based CellTiter-Glo cytotoxicity assay at 48-hour postexposure (**Figure 2B**). Although all these assays performed very similarly, it is important to note that the MTT and CellTiter-Glo assays both required individual sample sets to be prepared for each time point, whereas the substrate-free nature of the autobioluminescent cellular model system allowed for repeated monitoring of the same sample populations over time.
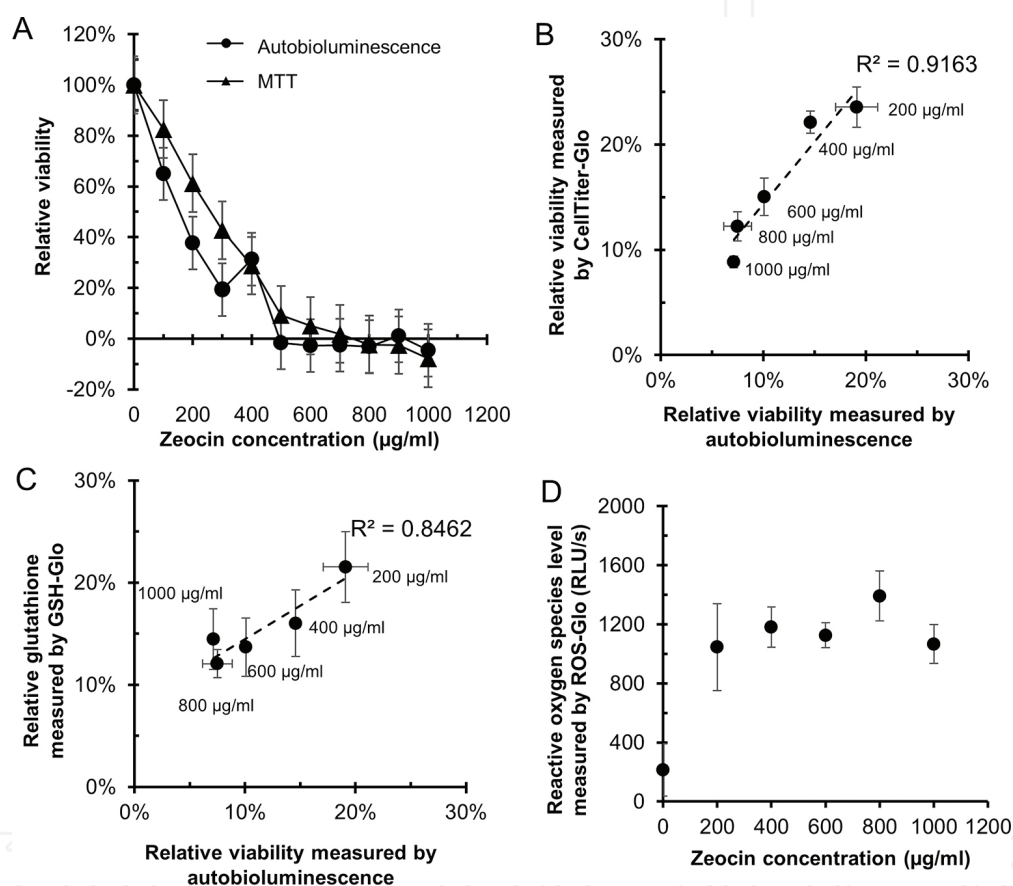
Figure 2. Correlating the data output of an autobioluminescent cellular model to alternative assay formats. (A) side-by-side comparison of the autobioluminescent model system output signal and the MTT cytotoxicity assay output for HEK293 cells exposed to 200–1000 μg/ml of Zeocin for 96 hours. (B) correlation of the relative viabilities of Zeocin-treated HEK293 cells as measured by autobioluminescence (*x*-axis) relative to those determined by the chemically stimulated bioluminescent CellTiter-Glo ATP content assay (*y*-axis). Each data point represents treatment with a unique dose of Zeocin. Relative viability was expressed as a percentage of the corresponding assay reading from untreated control cells. (C) correlation of the relative viabilities of Zeocin-treated HEK293 cells as measured by autobioluminescence (*x*-axis) relative to the chemically stimulated bioluminescent GSH-Glo glutathione concentration assay (*y*-axis). (D) treatment with 200–1000 μg/ml Zeocin resulted in an increase in reactive oxygen species levels in HEK293 cells that was not correlated to Zeocin concentration nor autobioluminescent output.

Furthermore, it was possible to leverage the nondestructive nature of the autobioluminescent HEK293 model to multiplex the real-time cytotoxicity assay with other downstream assays in

order to further elucidate the specific toxicity pathways that were activated. To illustrate this application, following evaluation for metabolic activity by autobioluminescent output, the cells were then immediately assayed to measure intracellular glutathione levels using a GSH-Glo assay or for the presence of reactive oxygen species using a ROS-Glo assay. In these evaluations, the GSH-Glo and ROS-Glo assays, respectively, identified a reduction in glutathione concentration and an increase in reactive oxygen species level, indicating oxidative stress. However, only the reduction in glutathione concentration was determined to be dose responsive, and correlated with the reduction in autobioluminescent output with an R^2 value of 0.8462 across the full range of compound exposure concentrations (200–1000 µg/ml) (**Figure 2C**). In contrast, reactive oxygen species levels were not observed to correlate with either the test compound concentrations or the autobioluminescent output (**Figure 2D**).

4. Variability of autobioluminescent responses resulting from system expression in different cellular hosts

## 4.1. Demonstrated autobioluminescent cellular model systems

Thus far, only four autobioluminescent cellular models have been demonstrated: human kidney cells (HEK293) [10, 18], human liver cells (HepG2), immortalized breast cancer cells (T-47D) [19, 32], and colorectal cancer cells (HCT116) [19]. The most well documented of these models has been the HEK293 cell line, which underwent validation by the National Institutes of Health as a pharmaceutical screening tool [25]. Less documentation is available for the T-47D, HepG2, and HCT116 cell lines; however, an analysis of their previous use has indicated that their average autobioluminescent output levels are lower than that of their autobioluminescent HEK293 counterpart [19], likely due to differences in their basal metabolic activity levels. Nonetheless, the signals from these alternative models have proven to be easily detectable [19], and their tumorigenic lineage has made them useful beyond the straightforward toxicology/metabolic activity screening applications that have emerged as the primary role for the autobioluminescent HEK293 model.

In particular, the autobioluminescent T-47D model has found utility as a biomonitor for the detection of endocrine disruptor activity due to its natural proliferative rate increase following estrogenic compound exposure. Since estrogenic compounds are defined by their stimulation of cell reproduction, this model has been harnessed to assay for increases in autobioluminescent output as a function of cellular proliferation to track a compound's ability to function as an endocrine disruptor using automated imaging equipment [19, 32]. In this role, autobioluminescent T-47D cells were shown to exhibit output signals proportional to their total population size (R^2 = 0.99) across a large dynamic range, suggesting that this model is appropriate for estimating the changes in population size stimulated by estrogenic responses. When challenged with picomolar concentrations of the prototypical estrogenic chemical, 17β-estradiol, a dose-dependent autobioluminescent response similar to traditional cell proliferation assays was observed [33]; however, contrary to the classical estrogenicity screens that require sample destruction, the autobioluminescent endocrine disruptor detection assay

maintained its trademark benefit of continuous data collection without sample sacrifice. This made the platform an efficient and universal screening system that offered the continuous detection of both cell toxicity and estrogenicity without the additional reagent costs tradition-ally associated with assay multiplexing.

4.2. Variability of autobioluminescent responses across differential cellular models

Because the autobioluminescent phenotype is closely related to the metabolic activity level of the host cell expressing the synthetic bacterial luciferase cassette, it is possible that significant variances in signal output potential can exist among available cellular models. This concern is compounded by the nascent state of the technology, which has limited the number of cellular hosts documented in the literature and made it difficult to determine how consistent the reporter signal output strength will be upon expression in previously untested cell lines or tissues. The uncertainty surrounding this variability is concerning given that choosing an appropriate cellular model is particularly crucial in drug discovery applications where the same compound can exert variable toxicological responses in different cell lines or tissue types [34]. Due to the lack of published data on this topic, experiments were performed to compare the autobioluminescent responses of the HEK293, T-47D, and HepG2 cell lines following exposure to the common chemotherapeutic agent doxorubicin. Due to the nondestructive, continuous nature of these autobioluminescent cellular models, it was possible to track the impact of doxorubicin exposure on metabolic activity dynamics over a 72-hour exposure period. In this example, a typical sigmoidal dose response was observed from the HEK293 cells at each assay time point with an estimated IC_{50} value of 2×10^{-8} M (20 nM) at 72-hour postex-posure (**Figure 3A**). However, doxorubicin treatment at concentrations higher than 5×10^{-7} M (500 nM) reduced autobioluminescent output by more than 95% within 72 hours of treatment. In contrast, both the T-47D and HepG2 models were less susceptible to doxorubicin than the HEK293 cells, and neither produced a sigmoidal dose response (**Figure 3B** and **C**). For these models, autobioluminescence reductions of greater than 95% were only observed by 72 hours following the start of doxorubicin treatment at concentrations ≥ 5 μM, whereas treatment with concentrations lower than 20 nM resulted in less than a 10% reduction in autobioluminescence output. Interestingly, however, doxorubicin treatment at 500 nM and 1 μM induced an increase
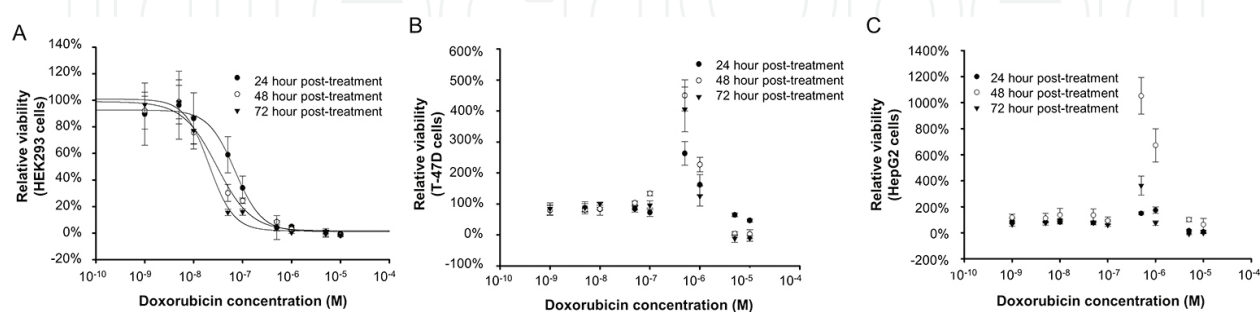
Figure 3. Variability of autobioluminescent dynamics in response to doxorubicin treatment across different cellular models. (A) autobioluminescent HEK293 cells displayed a sigmoidal dose-response curve in response to doxorubicin treatment at 24, 48, and 72 hours posttreatment. In contrast, neither (B) T-47D nor (C) HepG2 cells produced similar autobioluminescent responses to doxorubicin treatment over the course of the exposure period.

in autobioluminescent output in both the T-47D and HepG2 models over the course of the exposure period, with a peak at 48-hour posttreatment. These differential autobioluminescent responses are hypothesized to be the result of the varying cellular metabolic background activities and differential gene expression patterns exerted by each cell's activated toxicity pathways, thus demonstrating a clear emphasis on the importance of choosing a cellular model with an appropriate metabolic background for each specific application.

5. The use of autobioluminescent cellular models for three-dimensional cell culture applications

5.1. Common three-dimensional scaffold materials for *in vitro* drug discovery assays

Under natural *in vivo* conditions, cells reside in three-dimensional (3D) structures that are formed predominantly through attachment to an extracellular protein matrix. Partially through this attachment, the cells monitor and react to their immediate environment to modulate basic processes such as proliferation, morphology, and gene and protein expression, among other behaviors [35–37]. While in some cases, the natural proliferation rates and native phenotypes of the cells are retained under traditional monolayer culture conditions, more often their observed behavior and physiology become altered and are no longer representative of their natural *in vivo* characteristics [38]. In contrast, cells cultured in naturally derived or synthetically produced *in vitro* 3D culture systems have been demonstrated to better recapitulate *in vivo* cellular phenomena [39, 40]. Therefore, modern *in vitro* drug discovery platforms are increasingly taking advantage of synthetic 3D culture scaffolds to induce cellular growth under more *in vivo*-like conditions in order to improve the efficiency of novel compound development [41–43].

This transition has provided investigators with a variety of different 3D cell culture scaffold materials to choose from, many of which differ vastly in composition and, therefore, appropriateness to specific culture conditions. Collagen, a ubiquitous, naturally occurring protein polymer, has become frequently used for generalized *in vitro* 3D culture systems. The adaptability of collagen allows it to be used either on its own, as a hydrogel in which cells are suspended and then eventually attach to and remodel, or as a proteinaceous coating on other substrates [44]. Similar to collagen, other naturally occurring protein (e.g., fibrin or silks) and polysaccharide (e.g., chitin or hyaluronic acid) polymers have also been used alone, or in blends, to structure 3D cellular matrices [45] and affect cellular activities [46, 47]. In addition to these proteins, other natural materials such as corals have found utility as scaffolding for bone tissue engineering [48], as well as decellularized tissues repopulated with different cell types [49].

Synthetic polymers such as polycaprolactone, a comparatively basic example that is biodegradable and commonly used in medical applications, have also been widely applied toward 3D cell culture [50]. These synthetic 3D culture materials are becoming a popular option for *in vitro* drug discovery platforms due to their ability to be embedded with growth factors [51], specialized with functional groups, or studded with small molecules [52]. This generally offers

investigators more options for tailoring the physical characteristics of the final scaffold, such as fiber traits, meshed patterns, sponge surface area, void volume, and more precise control of the final physical design.

5.2. The advantages of autobioluminescent systems for cellular screening in three-dimensional cell culture applications

Both fluorescent and bioluminescent imaging systems are easily employed for interrogating cellular structures and activities in traditional monolayer cultures, but the utility of both is handicapped within 3D cell culture systems [26, 53]. Fluorescent reporters are limited primarily by the materials used in 3D culture systems, most of which display high levels of autofluorescence as the scaffold material responds to the excitation signal, or in some cases, to the presence of ambient light [54]. This effect manifests as strong background noise that can completely eclipse the desired signal and is especially prevalent for collagen or collagen-coated scaffolds, which display autofluorescence around 420–460 nm [54]. Further compounding the use of fluorescent technologies in 3D culture are the effects of phototoxicity and photobleaching. The repeated bombardment of samples with excitation photon energy has been shown to increase the prevalence of reactive oxygen species, which in turn can damage cellular components and skew assay results to the point where the cells may no longer be representative of their true *in vivo* state [55, 56]. Photobleaching, on the other hand, occurs when the fluorescent reporter is destroyed by the input photon energy and is no longer available to release photons. This attenuates the output signal and diminishes assay sensitivity, resulting in potential data misinterpretation. In addition to these cellular concerns, the 3D cell culture scaffold itself can also interfere with excitation by presenting a physical barrier to photon excitation at the interior of a construct that can be tens to hundreds of micrometers thick. To compensate for this, investigators must apply increased excitation intensities or durations to reach acceptable signal-to-noise ratios, which in turn increase the prevalence of autofluorescence, phototoxicity, and photobleaching.

Because of these multiple hurdles to using fluorescent reporters in 3D culture systems, bioluminescence has become more prevalent as an imaging system under these conditions [54, 57]. However, traditional chemically stimulated bioluminescent systems are similarly limited by the tendency of the 3D scaffold material to induce heterogeneous substrate distribution. Unlike monolayer cultures, where the activating chemical can be evenly distributed to all cells in a population, the presence of the 3D scaffold material, and the variations in construct size, cell density, and matrix configuration across the scaffold, results in the uneven distribution of the activating chemical and its required cosubstrates [58]. Consequently, cells on the exterior of the scaffold have more efficient access to the activating chemical than those on the interior and therefore can initiate a luminescent signal with altered timing and kinetics. This can lead to ambiguous bioluminescent measurements across the population of cells under study and misrepresentations of the true state of the system [36].

Unlike these fluorescent and chemically stimulated bioluminescent systems, autobioluminescent cellular models produce their luminescent signals independent of any external stimulation, and therefore are not subject to limitations imposed by activating chemical

diffusion dynamics, excitatory photon penetration, or phototoxicity and photobleaching. As a result, every cell in the population is continuously producing an autobioluminescent signal representative of its current metabolic activity level. Therefore, even if an asymmetric autobioluminescent signal is measured from a 3D construct, that distribution itself is of significant value to the investigator because it is an objective report on a cell's state at any given position in the construct. The primary physical limitation to the use of autobiolumi-nescent cellular models within 3D culture conditions is the physical absorption and dispersion of the autobioluminescent signal as it interacts with the structural material. As with the alternative systems, this can be mediated through the selection of amenable scaffolding material or by increasing signal acquisition times in order to obtain increased photon counts, although it cannot be completely eliminated as it is a fundamental limitation of the use of 3D structures within the culture system itself.

5.3. Using autobioluminescent cellular models to elucidate metabolic activity and drug responsiveness in monolayer and three-dimensional culture systems

The choice between a traditional monolayer and a 3D cell culture platform can strongly influence the basal metabolic activity of the cells under study. In monolayer formats, the metabolic state of the cells is constantly in flux as they are continuously passaged until senescence. In contrast, cells seeded into a natural or synthetic 3D scaffold may proliferate initially but, over time, their growth rate will slow and they will enter a stabilized metabolic equilibrium [42, 59]. This growth format is more representative of the cells' natural state, as their proliferation rates, morphology, and gene expression more closely resemble their *in vivo* states [41–43, 60]. However, the use of a 3D culture system does not guarantee faithful replication of *in vivo*-like conditions, as the 3D scaffold itself, through traits such as matrix stiffness or construct dimensions, can induce hypoxia at levels that differ significantly from those observed *in vivo* [61, 62]. These cases often better model tumor biology than healthy tissues, with the 3D construct mimicking a necrotic center with a proliferative exterior and a range of metabolic states in between [63]. Therefore, the direct comparison of metabolic activity levels (whether under a steady state, during proliferation, or throughout viability transitions) between scaffold types, traditional monolayer cultures, and *in vivo* cells can be complicated and should be made while considering factors like nutrient gradients, surface area, cell density, and relative perfusion rates, among many others.

Given the contrasting metabolic conditions between monolayer and 3D cell culture systems, autobioluminescent cellular models are uniquely positioned to assess cellular health in ways other imaging modalities cannot. Since autobioluminescent cells produce light as a function of their individual metabolic state without a dependence on externally supplied activating chemicals or excitatory photon stimulation, cross-platform comparisons can be performed with limited uncontrollable variability and using sample preparation scales that are logistically tractable. Indeed, an investigation of these contrasts using autobioluminescent HEK293 cells seeded onto polycaprolactone 3D culture scaffolds demonstrated a higher proliferation rate and basal metabolic activity level than when an identical number of cells was seeded and grown in monolayers on polystyrene plates or in suspension culture [64]. Similarly, when a

range of cellular concentrations were either plated in monolayers or encapsulated in collagen hydrogels and examined for autobioluminescence, only the output signals from the collagen-encapsulated 3D cultures remained tightly correlated with the initial cell density measurements after 48 hours of incubation. This suggests that, compared to traditional monolayer culture approaches, collagen-encapsulated 3D culture allows for longer term measurements of a wide range of cell population sizes.

Further interrogation indicated that the differences in basal metabolic levels induced by scaffold composition were significant enough to influence how the cells responded to xenobiotic challenges [42, 65], demonstrating that these emerging methods of 3D culture and adequate tools for evaluating cellular health are essential to modern drug discovery models. These results were not limited to only a single cell type, as breast, pancreatic and colon cancer cellular models all showed alterations to their proliferation and metabolic rates in the presence of stiffer 3D matrices, and were consequently found to be less sensitive to paclitaxel and gemcitabine treatment [62]. This was corroborated through a direct interrogation of collagen-encapsulated autobioluminescent HEK293 cells, which were observed to be more resistant to treatment with a metabolic inhibitor relative to their monolayer-grown counterparts. Together, these examples demonstrate how *in vitro* 3D culture alters cell behavior relative to traditional culture methods, and how investigators can use 3D culture variables to create better 3D models for drug discovery.

5.4. The use of autobioluminescent cellular models for continuous cellular tracking within three-dimensional culture scaffolds

Unlike fluorescent and chemically stimulated bioluminescent cellular models that require repeated, invasive stimulatory inputs to activate their output signals, autobioluminescent cellular models are amenable to continuous monitoring and dynamic metabolic activity tracking because their autobioluminescent output signals are continuously active. The on-demand availability and noninvasive nature of this output therefore makes these models highly amenable to repeated or continuous monitoring approaches that are not feasible with the traditional systems due to logistical or economical concerns. This offers significant utility for tumor xenograft tracking, which has traditionally relied upon repeated activating chemical injections, photonic stimulations, or physical measurements to track tumor volume, all of which are invasive and subject to large read-to-read variation [66, 67]. Autobioluminescent cellular models, in contrast, allow for low variation, high-resolution cellular tracking and viability monitoring.

As a demonstration of their utility for continuous monitoring, autobioluminescent HEK293 models have been grown on 3D polycaprolactone scaffolds and measured continuously for 24 hours via repeated light output measurements taken at 15-minute intervals using an automated system. Similarly, using magnetic-based 3D culture approaches, these same models have been monitored repeatedly for experiments lasting up to 45 days without the need to sacrifice samples or concerns related to sample-to-sample variability [64]. When employed in more complex *in vitro* 3D and xenograft models, the continuous signal generation of the autobioluminescent cellular models can be leveraged to provide data that was not previously obtainable,

such as monitoring cell detachment from 3D constructs to model tumor metastasis. This approach has significant value for therapeutic and regenerative medicine applications, where tracking stem cells after implantation is currently difficult to implement, but critical for model development [68]. In this application, autobioluminescent stem cell models could be employed to continuously monitor the site of implantation for changes in cell number or health. Then, from within the same sample or animal subject, sloughed cells could be visualized at peripheral sites, such as the brain, because the cells remain autobioluminescent. This approach would offer significant advantages over chemically stimulated bioluminescent systems, whose activating chemicals cannot be evenly distributed to all tissues and are restricted from the brain by the blood-brain barrier.

6. Advantages of autobioluminescent cellular models for assaying the metabolic effects of nontraditional stressors

The autobioluminescent system's ability to initiate and self-modulate its signal generation without cellular destruction or exogenous substrate input gives it the ability to function fully intracellularly, which is significantly different than the majority of *in vitro* bioluminescent assays that employ the presence of intracellular metabolites, usually in the form of ATP, to act as a limiting reagent for supporting the bioluminescent production of an exogenously applied luciferase and excess required alternative cosubstrates. Functionally, this means that autobio-luminescent systems can be utilized to monitor the metabolic activity or population size dynamics of specific community members in heterogeneous cocultures. This ability was recently investigated using cocultures of autobioluminescent HEK293 cells and virulent *Escherichia coli* O157:H7 to study the metabolic effects of bacterial infection and better under-stand the mechanism and timing of *E. coli* O157:H7 infection to improve treatment options for exposed patients [20].

In the course of this study, the autobioluminescent cellular system was compared to two other bioluminescence assays, the ATP-dependent CellTiter-Glo metabolic activity assay and the ROS-Glo hydrogen peroxide-dependent reactive oxygen species assay, in order to determine the most reliable method for assessing *E. coli* O157:H7 infection. Through the course of this evaluation, it was determined that the destructive assays were significantly influenced by the liberated metabolites from the co-lysed *E. coli* O157:H7 cells, which resulted in inflated readings due to overexposure of the exogenously supplemented luciferase reporter to the liberated bacterial metabolites. While the ATP-dependent CellTiter-Glo assay counterintui-tively showed an increase in metabolic activity concurrent with cellular death, raising from 58.4% of uninfected control cell bioluminescence at 2-hour postinfection (hpi) to 70.8% by 4 hpi, the autobioluminescent system was self-limited to reporting only on the metabolic dynamics of the targeted human cellular population, which were shown to decrease from 11.2% of control cell autobioluminescence at 2 hpi to 2.5% by 4 hpi. Similar results were observed in comparisons between the autobioluminescent cellular model and the ROS-Glo assay, although no significant differences in reporter function were observed when uninfected control cells were compared across all three reporter systems [19, 25].

Using the autobioluminescent cellular model, the investigators were able to determine the minimum bacterial population threshold required to induce reductions in host cell metabolic activity to between 5×10^5 and 1×10^6 colony forming units. Additionally, the authors were able to leverage the nondestructive nature of the autobioluminescent cellular model to monitor the ability of the host cells to recover from *E. coli* O157:H7 infection by tracking metabolic activity continuously as the infecting bacteria were removed and antibacterial compounds were applied. This analysis allowed them to conclude that the host cells could return to normal metabolic activity within 2 hours of bacterial clearance, even after infections were allowed to reduce the basal metabolic activity of the cells to 2.6% of the untreated control cells. This study serves as a demonstrative example of the way that the autobioluminescent system can be applied to obtain data that would not be logistically or economically feasible to obtain using traditional chemically stimulated bioluminescent systems due to the large number of samples, significant hands-on time, and high reagent costs that would be required.

7. Expression of autobioluminescence using alternative host systems

Although not directly relevant to drug discovery, it is nonetheless important to note the significantly larger body of autobioluminescent work that has been performed in nonhuman model systems. Because the autobioluminescent gene cassette used for this work is the same as the one used for human cellular expression, only with alternative supporting genetic elements and codon optimization, it is highly likely that the techniques developed in these alternative models will eventually make their way into the autobioluminescent human cellular models as well. Based on historical development patterns, it is likely that the most impending modification to be constructed will be a chemically activated promoter system for compound-specific activation of autobioluminescent output. This approach has been used in both bacterial and yeast-based autobioluminescent models to assess transcriptional activity from reporter system-fused promoters [69], to monitor autobioluminescently tagged populations in the environment [70], and to detect environmental pollutants for bioremediation [71, 72].

The classical examples of this system are the *Saccharomyces cerevisiae*-based autobioluminescent estrogen (BLYES) [4] and androgen (BLYAS) [73] detection strains. These strains do not produce any signal in the absence of their activating signals, but can self-initiate luciferase expression in response to compound detection through the use of estrogen and androgen response elements, respectively. Their use of autobioluminescence as a reporter allows them to respond substantially faster than the traditional *lacZ*-based colorimetric screens, offering detectable autobioluminescence within 1–6 hours of exposure [73] compared to the 24-hour performance period of alternative *lacZ*-based reporter systems [74]. Although no drug discovery assays using this expression strategy have yet been reported in human cellular systems, the ability to initiate autobioluminescent production in response to promoter activation has been demonstrated, suggesting that these model formats are on the horizon [19].

8. Conclusions

Although autobioluminescent cellular models are a new technology, they have emerged as promising tools for drug discovery. Their ability to reduce the number of required sample preparation steps and reagent requirements for existing assay formats positions them well to lower assay costs, while their high signal-to-noise ratios can allow them to fill the nondestructive imaging gaps left by fluorescent systems with complicating levels of background autofluorescence. Similarly, their natural compatibility to work within complex 3D culture systems should, at least in the near term, make them robust against the upcoming shift toward this growth system for early stage compound evaluation. However, their ultimate utility as drug discovery tools will rely on their adoption by the investigators routinely performing these assays. Without widespread use, and therefore sufficient validation within the field, it will be difficult for these models to take hold regardless of the advantages they offer.

Acknowledgements

Author details

Tingting Xu[1], Michael Conway[2], Ashley Frank[2], Amelia Brumbaugh[2], Steven Ripp[1] and Dan Close[2*]

*Address all correspondence to: dan.close@490biotech.com

1 Center for Environmental Biotechnology, The University of Tennessee, Knoxville, USA

2 BioTech, Knoxville, Tennessee, USA

References

[1] Herring PJ. Systematic distribution of bioluminescence in living organisms. Journal of Bioluminescence and Chemiluminescence. 1987;1(3):147–163.

[2] Close DM, Patterson SS, Ripp S, Baek SJ, Sanseverino J, Sayler GS. Autonomous bioluminescent expression of the bacterial luciferase gene cassette (*lux*) in a mammalian cell line. PLoS One. 2010;5(8):e12441.

[3] King JMH, Digrazia PM, Applegate B, Burlage R, Sanseverino J, Dunbar P, et al. Rapid, sensitive bioluminescent reporter technology for naphthalene exposure and biodegradation. Science. 1990;249(4970):778–781.

[4] Sanseverino J, Gupta RK, Layton AC, Patterson SS, Ripp SA, Saidak L, et al. Use of *Saccharomyces cerevisiae* BLYES expressing bacterial bioluminescence for rapid, sensitive detection of estrogenic compounds. Applied and Environmental Microbiology. 2005;71(8):4455–4460.

[5] Coutant EP, Janin YL. Synthetic routes to coelenterazine and other imidazo [1, 2-a] pyrazin-3-one luciferins: Essential tools for bioluminescence-based investigations. Chemistry—A European Journal. 2015;21(48):17158–17171.

[6] Close DM, Ripp S, Sayler GS. Reporter proteins in whole-cell optical bioreporter detection systems, biosensor integrations, and biosensing applications. Sensors. 2009;9(11):9147–9174.

[7] Close D, Ripp S, Sayler GS. Mammalian-based bioreporter targets: Protein expression for bioluminescent and fluorescent detection in the mammalian cellular background. In: Serra P, editor. Biosensors for Health, Environment and Biosecurity. Rijeka, Croatia: Intech; 2011. pp. 469–498.

[8] Sambrook J, Russell DW. Molecular Cloning: A Laboratory Manual. Cold Spring Harbor, New York: Cold Spring Harbor Laboratory Press; 2001.

[9] Gould SJ, Subramani S. Firefly luciferase as a tool in molecular and cell biology. Analytical Biochemistry. 1988;175(1):5–13.

[10] Patterson SS, Dionisi HM, Gupta RK, Sayler GS. Codon optimization of bacterial luciferase (*lux*) for expression in mammalian cells. Journal of Industrial Microbiology & Biotechnology. 2005;32:115–123.

[11] Almashanu S, Musafia B, Hadar R, Suissa M, Kuhn J. Fusion of *luxA* and *luxB* and its expression in *E. coli*, *S. cerevisiae* and *D. melanogaster*. Journal of Bioluminescence and Chemiluminescence. 1990;5(2):89–97.

[12] Escher A, O'Kane DJ, Lee J, Szalay AA. Bacterial luciferase alpha beta fusion protein is fully active as a monomer and highly sensitive *in vivo* to elevated temperature. Proceedings of the National Academy of Sciences of the United States of America. 1989;86(17):6528–6532.

[13] Kirchner G, Roberts JL, Gustafson GD, Ingolia TD. Active bacterial luciferase from a fused gene: Expression of a *Vibrio harveyi luxAB* translational fusion in bacteria, yeast and plant cells. Gene. 1989;81(2):349–354.

[14] Koncz C, Olsson O, Langridge WH, Schell J, Szalay AA. Expression and assembly of functional bacterial luciferase in plants. Proceedings of the National Academy of Sciences of the United States of America. 1987;84(1):131–135.

[15] Olsson O, Escher A, Sandberg G, Schell J, Koncz C, Szalay AA. Engineering of monomeric bacterial luciferase by fusion of *luxA* and *luxB* genes in *Vibrio harveyi*. Gene. 1989;81(2):335–347.

[16] Pazzagli M, Devine JH, Peterson DO, Baldwin TO. Use of bacterial and firefly luciferases as reporter genes in DEAE-dextran-mediated transfection in mammalian cells. Analytical Biochemistry. 1992;204(2):315–323.

[17] Westerlund-Karlsson A, Saviranta P, Karp M. Generation of thermostable monomeric luciferases from *Photorhabdus luminescens*. Biochemical and Biophysical Research Communications. 2002;296(5):1072–1076.

[18] Close DM, Patterson SS, Ripp SA, Baek SJ, Sanseverino J, Sayler GS. Autonomous bioluminescent expression of the bacterial luciferase gene cassette (*lux*) in a mammalian cell line. PLoS One. 2010;5(8):e12441.

[19] Xu T, Ripp SA, Sayler GS, Close DM. Expression of a humanized viral 2A-mediated *lux* operon efficiently generates autonomous bioluminescence in human cells. PLoS One. 2014;9(5):e96347.

[20] Xu T, Marr E, Lam H, Ripp S, Sayler G, Close D. Real-time toxicity and metabolic activity tracking of human cells exposed to *Escherichia coli* O157:H7 in a mixed consortia. Ecotoxicology. 2015;24(10):2133–2140.

[21] Shaner NC, Steinbach PA, Tsien RY. A guide to choosing fluorescent proteins. Nature Methods. 2005;2(12):905–909.

[22] Close DM, Ripp SA, Sayler GS. Reporter proteins in whole-cell optical bioreporter detection systems, biosensor integrations, and biosensing applications. Sensors. 2009;9(11):9147–9174.

[23] Thorne N, Inglese J, Auld DS. Illuminating insights into firefly luciferase and other bioluminescent reporters used in chemical biology. Chemistry & Biology. 2010;17(6):646–657.

[24] Xu T, Close D, Handagama W, Marr E, Sayler G, Ripp S. The expanding toolbox of *in vivo* bioluminescent imaging. Frontiers in Oncology. 2016;6:150.

[25] Class B, Thorne N, Aguisanda F, Southall N, Mckew J, Zheng W. High-throughput viability assay using an autonomously bioluminescent cell line with a bacterial *lux* reporter. Journal of Laboratory Automation. 2015;20(2):164–174.

[26] Close DM, Hahn RE, Patterson SS, Ripp SA, Sayler GS. Comparison of human optimized bacterial luciferase, firefly luciferase, and green fluorescent protein for contin-

uous imaging of cell culture and animal models. Journal of Biomedical Optics. 2011;16(4):e12441.

[27] Choy G, O'Connor S, Diehn FE, Costouros N, Alexaner HR, Choyke P, et al. Comparison of noninvasive fluorescent and bioluminescent small animal optical imaging. Biotechniques. 2003;35(5):1022–1030.

[28] Troy T, Jekic-McMullen D, Sambucetti L, Rice B. Quantitative comparison of the sensitivity of detection of fluorescent and bioluminescent reporters in animal models. Molecular Imaging. 2004;3(1):9–23.

[29] Welsh DK, Kay SA. Bioluminescence imaging in living organisms. Current Opinion in Biotechnology. 2005;16(1):73–78.

[30] Dehdashti SJ, Zheng W, Gever JR, Wilhelm R, Nguyen DT, Sittampalam G, et al. A high-throughput screening assay for determining cellular levels of total tau protein. Current Alzheimer Research. 2013;10(7):679–687.

[31] Zhao H, Doyle TC, Coquoz O, Kalish F, Rice BW, Contag CH. Emission spectra of bioluminescent reporters and interaction with mammalian tissue determine the sensitivity of detection *in vivo*. Journal of Biomedical Optics. 2005;10(4):41210.

[32] Xu T, Close DM, Webb JD, Price SL, Ripp SA, Sayler GS. Continuous, real-time bioimaging of chemical bioavailability and toxicology using autonomously bioluminescent human cell lines. In: SPIE-Sensing Technologies for Global Health, Military Medicine, Disaster Response and Environmental Monitoring III; 29 April–3 May, 2013. Baltimore, Maryland, USA. Berlingham, Washington: SPIE; 2013. p. 872310.

[33] Soto AM, Maffini MV, Schaeberle CM, Sonnenschein C. Strengths and weaknesses of *in vitro* assays for estrogenic and androgenic activity. Best Practice & Research Clinical Endocrinology & Metabolism. 2006;20(1):15–33.

[34] Holliday DL, Speirs V. Choosing the right cell line for breast cancer research. Breast Cancer Research. 2011;13(4):215–215.

[35] Khalil AA, Jameson MJ, Broaddus WC, Lin PS, Dever SM, Golding SE, et al. The influence of hypoxia and pH on bioluminescence imaging of luciferase-transfected tumor cells and xenografts. International Journal of Molecular Imaging. 2013;2013:9.

[36] Lambrechts D, Roeffaers M, Goossens K, Hofkens J, Vande Velde G, Van de Putte T, et al. A causal relation between bioluminescence and oxygen to quantify the cell niche. PLoS One. 2014;9(5):e97572.

[37] Kleinman HK, Philp D, Hoffman MP. Role of the extracellular matrix in morphogenesis. Current Opinion in Biotechnology. 2003;14(5):526–532.

[38] Pampaloni F, Reynaud EG, Stelzer EH. The third dimension bridges the gap between cell culture and live tissue. Nature Reviews Molecular Cell Biology. 2007;8(10):839–845.

[39] Berthiaume F, Moghe PV, Toner M, Yarmush ML. Effect of extracellular matrix topology on cell structure, function, and physiological responsiveness: Hepatocytes cultured in a sandwich configuration. The FASEB Journal. 1996;10(13):1471–1484.

[40] Cukierman E, Pankov R, Stevens DR, Yamada KM. Taking cell-matrix adhesions to the third dimension. Science. 2001;294(5547):1708–1712.

[41] Nam KH, Smith AS, Lone S, Kwon S, Kim DH. Biomimetic 3D tissue models for advanced high-throughput drug screening. Journal of Laboratory Automation. 2015;20(3):201–215.

[42] Edmondson R, Broglie JJ, Adcock AF, Yang L. Three-dimensional cell culture systems and their applications in drug discovery and cell-based biosensors. Assay and Drug Development Technologies. 2014;12(4):207–218.

[43] Breslin S, O'Driscoll L. Three-dimensional cell culture: The missing link in drug discovery. Drug Discovery Today. 2013;18(5–6):240–249.

[44] Chevallay B, Herbage D. Collagen-based biomaterials as 3D scaffold for cell cultures: Applications for tissue engineering and gene therapy. Medical & Biological Engineering & Computing. 2000;38(2):211–218.

[45] Taylor PM. Biological matrices and bionanotechnology. Philosophical Transactions of the Royal Society of London B: Biological Sciences. 2007;362(1484):1313–1320.

[46] Ruedinger F, Lavrentieva A, Blume C, Pepelanova I, Scheper T. Hydrogels for 3D mammalian cell culture: A starting guide for laboratory practice. Applied Microbiology and Biotechnology. 2015;99(2):623–636.

[47] Caliari SR, Burdick JA. A practical guide to hydrogels for cell culture. Nature Methods. 2016;13(5):405–414.

[48] Hou R, Chen F, Yang Y, Cheng X, Gao Z, Yang HO, et al. Comparative study between coral-mesenchymal stem cells-rhBMP-2 composite and auto-bone-graft in rabbit critical-sized cranial defect model. Journal of Biomedical Materials Research Part A. 2007;80(1):85–93.

[49] Hoshiba T, Lu H, Kawazoe N, Chen G. Decellularized matrices for tissue engineering. Expert Opinion on Biological Therapy. 2010;10(12):1717–1728.

[50] Dash TK, Konkimalla VB. Poly-ɛ-caprolactone based formulations for drug delivery and tissue engineering: A review. Journal of Controlled Release. 2012;158(1):15–33.

[51] Cetinkaya G, Turkoglu H, Arat S, Odaman H, Onur MA, Gumusderelioglu M, et al. LIF-immobilized nonwoven polyester fabrics for cultivation of murine embryonic stem cells. Journal of Biomedical Materials Research Part A. 2007;81(4):911–919.

[52] Vasita R, Katti DS. Nanofibers and their applications in tissue engineering. International Journal of Nanomedicine. 2006;1(1):15–30.

[53] White NS, Errington RJ. Fluorescence techniques for drug delivery research: Theory and practice. Advanced Drug Delivery Reviews. 2005;57(1):17–42.

[54] Smith LE, Smallwood R, Macneil S. A comparison of imaging methodologies for 3D tissue engineering. Microscopy Research and Technique. 2010;73(12):1123–1133.

[55] Daddysman MK, Tycon MA, Fecko CJ. Photoinduced damage resulting from fluorescence imaging of live cells. Methods in Molecular Biology. 2014;1148:1–17.

[56] Magidson V, Khodjakov A. Circumventing photodamage in live-cell microscopy. Methods in Cell Biology. 2013;114:545–560.

[57] Michelini E, Cevenini L, Calabretta MM, Calabria D, Roda A. Exploiting *in vitro* and *in vivo* bioluminescence for the implementation of the three Rs principle (replacement, reduction and refinement) in drug discovery. Analytical and Bioanalytical Chemistry. 2014;406(23):5531–5539.

[58] Malda J, Klein TJ, Upton Z. The roles of hypoxia in the *in vitro* engineering of tissues. Tissue Engineering. 2007;13(9):2153–2162.

[59] Wrzesinski K, Rogowska-Wrzesinska A, Kanlaya R, Borkowski K, Schwammle V, Dai J, et al. The cultural divide: Exponential growth in classical 2D and metabolic equilibrium in 3D environments. PLoS One. 2014;9(9):e106973.

[60] Birgersdotter A, Sandberg R, Ernberg I. Gene expression perturbation *in vitro*—A growing case for three-dimensional (3D) culture systems. Seminars in Cancer Biology. 2005;15(5):405–412.

[61] Pruksakorn D, Lirdprapamongkol K, Chokchaichamnankit D, Subhasitanont P, Chiablaem K, Svasti J, et al. Metabolic alteration of HepG2 in scaffold-based 3-D culture: Proteomic approach. Proteomics. 2010;10(21):3896–3904.

[62] Fang JY, Tan SJ, Wu YC, Yang Z, Hoang BX, Han B. From competency to dormancy: A 3D model to study cancer cells and drug responsiveness. Journal of Translational Medicine. 2016;14:38.

[63] Mehta G, Hsiao AY, Ingram M, Luker GD, Takayama S. Opportunities and challenges for use of tumor spheroids as models to test drug delivery and efficacy. Journal of Controlled Release. 2012;164(2):192–204.

[64] Webb JD. Evaluation of novel multi-dimensional tissue culturing methods using autonomously bioluminescent human cell lines [thesis]. Knoxville: The University of Tennessee; 2014.

[65] LaBonia GJ, Lockwood SY, Heller AA, Spence DM, Hummon AB. Drug penetration and metabolism in 3D cell cultures treated in a 3D printed fluidic device: Assessment of irinotecan via MALDI imaging mass spectrometry. Proteomics. 2016;16(11–12):1814–1821.

[66] Tomayko MM, Reynolds CP. Determination of subcutaneous tumor size in athymic (nude) mice. Cancer Chemotherapy and Pharmacology. 1989;24(3):148–154.

[67] Jenkins DE, Oei Y, Hornig YS, Yu SF, Dusich J, Purchio T, et al. Bioluminescent imaging (BLI) to improve and refine traditional murine models of tumor growth and metastasis. Clinical and Experimental Metastasis. 2003;20(8):733–744.

[68] von der Haar K, Lavrentieva A, Stahl F, Scheper T, Blume C. Lost signature: Progress and failures in *in vivo* tracking of implanted stem cells. Applied Microbiology and Biotechnology. 2015;99(23):9907–9922.

[69] Engebrecht J, Simon M, Silverman M. Measuring gene expression with light. Science. 1985;227(4692):1345–1347.

[70] de Weger LA, Dunbar P, Mahafee WF, Lugtenberg BJJ, Sayler GS. Use of bioluminescence markers to detect *Pseudomonas* spp. in the rhizosphere. Applied and Environmental Microbiology. 1991;57(12):3641–3644.

[71] Ripp S, Nivens DE, Ahn Y, Werner C, Jarrell J, Easter JP, et al. Controlled field release of a bioluminescent genetically engineered microorganism for bioremediation process monitoring and control. Environmental Science & Technology. 2000;34(5):846–853.

[72] Xu T, Close D, Smartt A, Ripp S, Sayler G. Detection of organic compounds with whole-cell bioluminescent bioassays. In: Thouand G, Marks R, editors. Bioluminescence: Fundamentals and Applications in Biotechnology, Volume 1. Advances in Biochemical Engineering/Biotechnology. 144. Berlin, Heidelberg: Springer; 2014. pp. 111–151.

[73] Eldridge M, Sanseverino J, Layton A, Easter J, Schultz T, Sayler G. *Saccharomyces cerevisiae* BLYAS, a new bioluminescent bioreporter for detection of androgenic compounds. Applied and Environmental Microbiology. 2007;73(19):6012–6018.

[74] Gaido KW, Leonard LS, Lovell S, Gould JC, Babai D, Portier CJ, et al. Evaluation of chemicals with endocrine modulating activity in a yeast-based steroid hormone receptor gene transcription assay. Toxicology and Applied Pharmacology. 1997;143(1): 205–212.